Biosensors and Bioelectronics 24 (2009) 1765–1770

Contents lists available at ScienceDirect

Biosensors and Bioelectronics

journal homepage: www.elsevier.com/locate/bios

Preparation of gold nanoparticles/functionalized multiwalled carbon nanotube nanocomposites and its glucose biosensing application

Fenghua Li[a], Zhonghua Wang[b], Changsheng Shan[a], Jiangfeng Song[a], Dongxue Han[a], Li Niu[a,*]

[a] State Key Laboratory of Electroanalytical Chemistry, Changchun Institute of Applied Chemistry, and Graduate University of the Chinese Academy of Sciences, Chinese Academy of Sciences, Renmin St. 5625, Changchun 130022, PR China
[b] Laboratory of Fiber Materials and Modern Textile, Growing Base for State Key Laboratory, Qingdao University, Qingdao 266071, PR China

ARTICLE INFO

Article history:
Received 19 June 2008
Received in revised form 3 September 2008
Accepted 4 September 2008
Available online 18 September 2008

Keywords:
Multiwalled carbon nanotubes
Ionic liquids
Gold nanoparticles
Electrocatalysis
Biosensors

ABSTRACT

Gold nanoparticles stabilized by amino-terminated ionic liquid (Au-IL) have been *in situ* noncovalently deposited on poly(sodium 4-styrene-sulfonate) (PSS)-functionalized multiwalled carbon nanotubes (MWCNTs) to form a MWCNTs/PSS/Au-IL nanocomposite. PSS can interact with MWCNTs through hydrophobic interaction. Amino-terminated ionic liquid was applied to reduce aqueous $HAuCl_4$, and the resulting gold nanoparticles were attached to the PSS-functionalized MWCNTs simultaneously. Most gold nanoparticles dispersed well on the functionalized MWCNTs. Transmission electron microscopy, Raman and X-ray photoelectron spectroscopy were used to confirm the composition and structure of the nanocomposites. The resulting MWCNTs/PSS/Au-IL composite exhibits good electrocatalysis toward oxygen and hydrogen peroxide reduction. And good biocompatibility with glucose oxidase was also demonstrated due to its good biocatalysis toward glucose substrate, which offered a friendly environment for the immobilization of biomolecules. Such bionanocomposite provides us potential applications in fabrication of biosensors. The resulting biosensor exhibits good response to glucose with a low detection limit 25 μM. It also has excellent reproducibility, satisfied operational stability and good storage stability.

1. Introduction

Since the discovery of carbon nanotubes (CNTs) (Iijima, 1991), CNTs-based nanocomposites have been intensively studied due to their potential applications in catalysis, chemical sensors, hydrogen storage, power storage, and drug loading and delivery, etc. (Harris, 2004; Wildgoose et al., 2006; Liu et al., 2007). Despite its insolubility in most commonly used solvents, some progress toward their chemical processing and wrapping with polymers have recently been achieved (O'Connell et al., 2002; Correa-Duarte et al., 2004). In addition, in order to extend the potential applications of CNTs, it is essential to modify the inert sidewalls by chemical functionalization and/or attach suitable nanostructures to the nanotubes (Jiang et al., 2003). Especially, the attachment of gold nanoparticles to CNT sidewalls shows particularly great promise toward novel, highly efficient photoelectrochemical cells, fuel cells, and sensor devices. Therefore, a number of approaches have been suggested to prepare CNT/gold nanohybrids, such as sol–gel technique (Zhang et al., 2003), conventional impregnation method (Han et al., 2004), chemical vapor deposition (Xue et al., 2001), solution growth (Kim et al., 2006), and so on.

Ionic liquids (ILs) have attracted a great deal of interests due to their numerous advantages over conventional solvents such as negligible vapor pressures, a wide range of viscosities, high chemical and thermal stability, high conductivity and wide electrochemical window, etc. (Lee, 2006). They also have tremendous potential in organic synthesis (Mehnert et al., 2002), green chemistry (Anderson and Armstrong, 2005), separations (Gholap et al., 2003), spectroscopy (Schäfer et al., 2005), and electrochemistry (Shen et al., 2007). Recently, Au nanoparticles reduced and/or stabilized by ionic liquids have been synthesized and shown their unique properties (Itoh et al., 2004; Tatumi and Fujihara, 2005). Recently, some systems consisting of CNTs (Deng et al., 2008), CNTs/Au nanoparticles (Cui et al., 2008; Wu et al., 2007), or IL/graphite material (Musameh et al., 2008) have been applied in biosensors and got good results. However, as far as we know, hybrid composites based on the CNTs/Au atoms/IL are a few.

In our group, 1-(3-aminopropyl)-3-methylimidazolium bromide, an amino-terminated ionic liquid (IL-NH_2) has been synthesized and covalently modified on CNTs (Zhang et al., 2006), and even applied to simultaneously reduce $HAuCl_4$ solution and further stabilize the gold nanoparticles.

* Corresponding author. Tel.: +86 431 8526 2425; fax: +86 431 8526 2800.
E-mail address: lniu@ciac.jl.cn (L. Niu).

0956-5663/$ – see front matter © 2008 Elsevier B.V. All rights reserved.
doi:10.1016/j.bios.2008.09.005

Here, this work introduced an *in situ* route to prepare multiwalled carbon nanotubes/polymer/gold-ionic liquid (MWCNTs/PSS/Au-IL) composites. The mean diameter of Au nanoparticles is 2.87 nm, which covered uniformly on MWCNTs/PSS surface. And its electrocatalysis and biocompatibility are also explored further in this work.

2. Experimental

2.1. Reagents

MWCNTs prepared by chemical vapor deposition (CVD) were purchased from Shenzhen Nanotech Port Ltd. Co. (China). 1-methylimidazole (≥98%, Linhai Kaile Chemicals, China) was distilled at reduced pressure before use. $HAuCl_4{\cdot}4H_2O$ (99.9+%, Aldrich), 3-bromopropylamine hydrobromide (98%, Aldrich), poly(sodium 4-styrene-sulfonate) (PSS) (typical M_w 70,000, Aldrich), glucose oxidase from *Aspergillus niger* (100,000–250,000 units/g, Sigma), hydrogen peroxide (30%, Beijing Chemicals, China), potassium dihydrogen phosphate (≥99.5%, Beijing Chemicals, China), di-sodium hydrogen phosphate (≥99.0%, Laiyan Chemicals, China), ethanol (99.8%, Beijing Chemicals, China), HNO_3 (65%, Beijing Chemicals, China), H_2SO_4 (98%, Beijing Chemicals, China) and ethyl acetate (99.7%, Beijing Chemicals, China) were used as received. All aqueous solutions were prepared with ultrapure water (>18 MΩ) obtained from a Milli-Q Plus system (Millipore).

2.2. Synthesis of IL-NH_2

IL-NH_2 was prepared following our previous report (Zhang et al., 2006). Briefly, 3.32 g 3-bromopropylamine hydrobromide and 1.20 mL of 1-methylimidazole were added to 37.5 mL ethanol, forming a colourless solution which was refluxed under nitrogen for 24 h. The resulting turbid mixture was purified by re-crystallization and then the resulting white product was dried for 24 h at 60 °C under vacuum.

2.3. Preparation of MWCNTs/PSS/Au-IL and MWCNTs/PSS/IL composites

Scheme 1 shows an illustration of the preparation of MWCNTs/PSS/Au-IL nanocomposites. The as-received MWCNTs were treated with a 1:3, v/v mixture of HNO_3 (65%) and H_2SO_4 (98%) for 2 h with continuous ultrasonication. The product was centrifuged, washed with ultrapure water until its pH approaching 7. After being dried, polymer wrapping was performed by means of a variation of the method reported by O'Connell et al. (2001). 10.5 mg purified MWCNTs and 0.70 g PSS were dispersed in 70 mL distilled water with continuous sonication for 15 min, then held at 50 °C for 12 h under vigorous agitation. Excess PSS was removed by three centrifugation/redispersion cycles, spinning at 12,000 rpm for 30 min. The product was dried under vacuum at 60 °C overnight to get MWCNTs/PSS powder.

0.042 g IL-NH_2 was dissolved in 11.60 mL ultrapure water, then 0.20 mL MWCNTs/PSS aqueous solution (2 mg/mL) was added dropwise into the mixture under stirring to form a well-dispersed solution. Then 0.20 mL of 0.02 mol/L $HAuCl_4$ aqueous solution was added dropwise over several minutes. After stirring for 10 h, the product was subsequently filtered through a Nylon membrane with 0.22 μm pores, thoroughly washed with water and then dried overnight at 60 °C under vacuum.

The preparation of MWCNTs/PSS/IL composites was the same with the preparation of MWCNTs/PSS/Au-IL just without the addition of $HAuCl_4$ aqueous solution.

2.4. Preparation of MWCNTs/PSS, MWCNTs/PSS/IL, MWCNTs/PSS/Au-IL, MWCNTs/PSS/GOD, MWCNTs/PSS/IL/GOD and MWCNTs/PSS/Au-IL/GOD composite films

The GC (3 mm in diameter) electrode was polished subsequently with 1.0, 0.3 and 0.05 μm alumina slurry, and sonicated in water for several times. To prepare MWCNT/PSS-modified, MWCNTs/PSS/IL-modified, MWCNTs/PSS/Au-IL-modified GC electrodes, an aliquot of 2 μL of 2 mg/mL MWCNT/PSS, MWCNTs/PSS/IL,

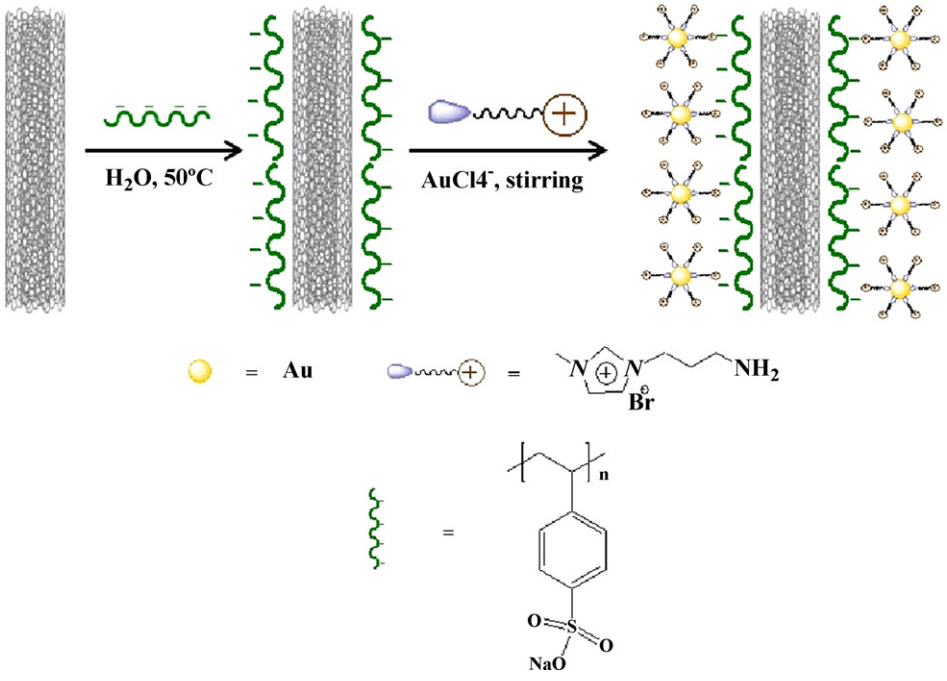

Scheme 1. Illustration of the preparation of MWCNTs/PSS/Au-IL nanocomposites.

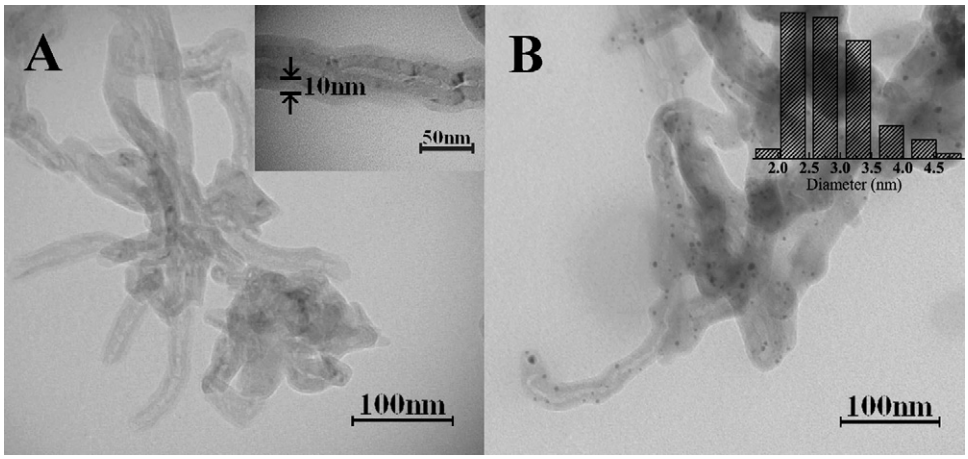

Fig. 1. TEM images of (A) MWCNTs/PSS composites, the PSS layer on the MWCNTs walls is ca. 10 nm (inset) and (B) MWCNTs/PSS/Au-IL nanocomposites, particle size distribution as inset.

MWCNTs/PSS/Au-IL aqueous solution were coated on the pretreated GC electrodes with a microsyringe, respectively, and then dried for 24 h in air before use. In order to prepare MWCNTs/PSS/GOD, MWCNTs/PSS/IL/GOD, MWCNTs/PSS/Au-IL/GOD composite film, 10 μL of 3 mg/mL GOD PBS solution were dropped on the dry MWCNTs/PSS-modified, MWCNTs/PSS/IL-modified, MWCNTs/PSS/Au-IL-modified GC electrodes, respectively, then dried for ca. 24 h at 4 °C.

2.5. Instruments and measurements

Transmission electron microscopy (TEM) image was taken with JEOL 2000 transmission electron microscope operating at 200 kV. Fourier transform infrared spectra (FTIR) were recorded using a Bruker Tensor 27 Spectrometer. Raman spectra were collected using a Renishaw 2000 system with an Argon ion laser (514.5 nm) and charge-coupled device detector. X-ray photoelectron spectroscopy (XPS) analysis was carried out on an ESCALAB MK II X-ray photoelectron spectrometer. Cyclic voltammetry scans were performed using a CHI660 electrochemical workstation (CHI, USA).

3. Results and discussion

3.1. Structure characterization

FTIR spectra of PSS, activated nanotubes and MWCNTs/PSS were recorded, respectively (shown in Supplementary data, Fig. S1). In MWCNTs-COOH (curve b), peaks at ca. 1715 and 1580 cm^{-1} can be assigned to the carboxylic C=O bond (Park et al., 2006) and the asymmetric C=C stretching vibration in the graphene sheet (Jiang et al., 2007), respectively. The characteristic peaks of MWCNTs-COOH and PSS are all observed in the spectrum of the MWCNTs/PSS composite and shifted to much lower wavenumbers (curve a and c). FTIR peaks at ca. 1715 and 1580 cm^{-1} are shifted to 1708 and 1568 cm^{-1}, respectively, which might be attributed to the favorable interaction between MWCNTs and PSS. Peaks at ca. 1157 and 1104 cm^{-1} are assigned to O=S=O stretching vibrations in $-SO_3H$ and the asymmetric O=S=O stretching vibration in SO_3^- in PSS component, respectively (Jamróz and Maréchal, 2005). According to previous report (Wang et al., 2008), the red-shift of PSS characteristic peaks may be resulted from the doping effect of SO_3^-.

As shown in Fig. 1A, the MWCNTs were fully wrapped by PSS, which resulted negative charges on the tube surface and enhanced solubilization of the MWCNTs. From the amplification image (inset in Fig. 1A), it can be obviously distinguished that the PSS layer on the MWCNTs walls was ca. 10 nm. After immobilization of ionic liquid-functionalized Au nanoparticles, the resulting TEM image revealed that spherical Au particles are present with fairly even, non-ordered distribution along the walls and at the ends of nanotubes (Fig. 1B). The Au nanoparticles ranged from 1.84 to 4.74 nm in diameter (with mean diameter 2.87 nm obtained from inset of Fig. 1B).

Raman spectra of the MWCNT-COOH, MWCNTs/PSS, and MWCNTs/PSS/Au-IL nanocomposites were shown in the supporting information (Supplementary data, Fig. S2). The D-band and G-band (Cui et al., 2005) of carbon nanotubes were observed, which was associated with the defect-related mode and the graphitic hexagon-pinch mode, respectively. The D-band and G-band shift to higher wavenumbers for MWCNTs/PSS/Au-IL nanocomposites. The PSS wrapping of the MWCNT-COOH decreased the ratio of the D-band to the G-band (*R*-value) from 1.108 to 1.072, which indicated that some defects disappeared after the PSS wrapping. With further IL-NH_2 reduction of Au nanoparticles on PSS-functionalized MWCNTs, the *R*-value was reduced to 1.107, indicating that regeneration of defects with the growth of Au nanoparticles. This upshift in the D-band and G-band and the reduction of the *R*-value from MWCNTs/PSS to MWCNTs/PSS/Au-IL nanocomposite should be related to the interactions between MWCNTs/PSS and deposited Au atoms (Kim et al., 2007).

Fig. 2 shows the XPS spectrum of MWCNTs/PSS/Au-IL composites. Top-right inset shows a single S 2p peak at 168.5 eV with a full

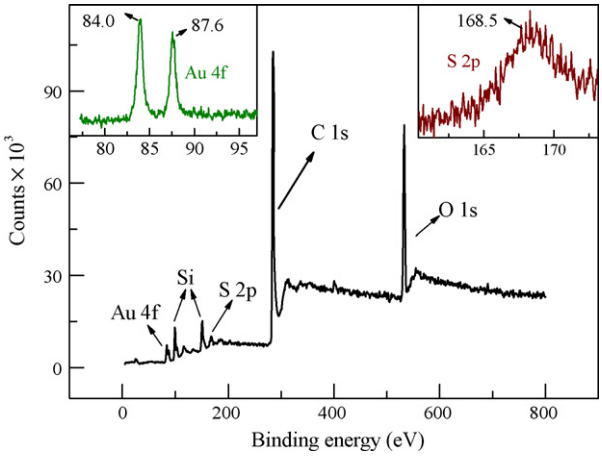

Fig. 2. XPS spectrum of MWCNTs/PSS/Au-IL composites. Insets: the Au 4f doublet (top-left) and S 2p (top-right).

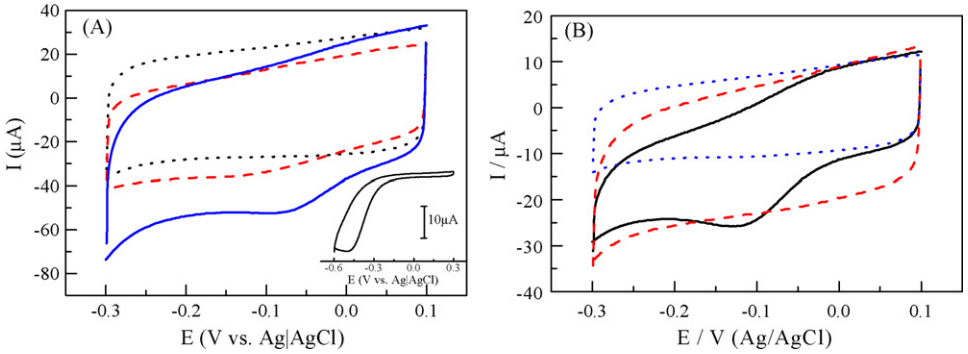

Fig. 3. (A) CV grams of MWCNTs/PSS/Au-IL-modified GC electrode in 0.5 M H_2SO_4 solution saturated with O_2 (solid) and N_2 (dotted); MWCNTs/PSS-modified electrode in 0.5 M H_2SO_4 solution saturated with O_2 (dashed). Inset: bare GC electrode in 0.5 M H_2SO_4 solution saturated with O_2. (B) CV grams of MWCNTs/PSS/Au-IL-modified GC electrode in 0.5 M N_2-saturated H_2SO_4 solution without (dotted) and with 5 mM H_2O_2 (solid); MWCNTs/PSS-modified electrode in 0.5 M N_2-saturated H_2SO_4 solution containing 5 mM H_2O_2 (dashed). Scan rate: 0.05 V s^{-1}.

width at half-maximum (fwhm) of 2.63 eV, which is consistent with the $-SO_3H$ state (Smith et al., 2004), confirming the PSS wrapping layer formed on the MWCNTs walls. The Au $4f_{7/2}$ and Au $4f_{5/2}$ peaks originated from the deposited Au nanoparticles on the carbon nanotubes reduced by amino-terminated ionic liquid that appeared at ca. 84.0 and 87.6 eV (peak-to-peak distance of 3.6 eV), respectively (Jaramillo et al., 2003).

3.2. Electrocatalytical properties

MWCNTs/PSS/Au-IL, MWCNTs/PSS-modified and bare GC electrodes were used to explore their electrochemical characteristics. As shown in Fig. 3A, a well-defined peak (solid) was present at ca. −0.091 V at the MWCNTs/PSS/Au-IL-modified GC electrode in the O_2-saturated solution, while no peak was seen in the N_2-saturated solution (dotted). A slight O_2 reduction at MWCNTs/PSS-modified GC electrode was ca. −0.142 V (dashed). Moreover, the oxygen reduction peak at bare GC electrode was at ca. −0.50 V (as shown as inset). The 409 mV positive shift achieved at the MWCNTs/PSS/Au-IL-modified electrode compared to bare GC electrode indicated significant electrocatalytic activity of MWCNTs/PSS/Au-IL nanocomposites toward the reduction of oxygen. As shown in Fig. 3B, the reduction peak of H_2O_2 at the MWCNTs/PSS/Au-IL-modified GC electrode was also detected (solid). A slight H_2O_2 was reduced at MWCNTs/PSS-modified GC electrode too (dashed). Therefore, the above results clearly indicated that MWCNTs/PSS/Au-IL nanocomposites could electrocatalytically reduce O_2 and H_2O_2 to H_2O, which was in favor of further utilization of glucose sensing.

3.3. Biocompatibility and glucose biosensing

The cyclic voltammograms of a MWCNTs/PSS/Au-IL-modified and MWCNTs/PSS/Au-IL/GOD-modified GC electrodes in 0.05 M N_2-saturated PBS (pH 7.0) solution are shown as curve e and f in Fig. 4A, respectively. It is clear to see that no observable voltammetric response can be obtained at the MWCNTs/PSS/Au-IL modification, but a pair of well-defined redox peaks can be obviously achieved at the MWCNTs/PSS/Au-IL/GOD modification, which might be ascribed to the redox reaction of the prosthetic group (FAD) bound to the GOD (Jiang et al., 1995). Fig. 4B shows CV curves of the MWCNTs/PSS/Au-IL/GOD at various scan rates. The peak currents increased linearly with scan rates (up to 0.2 V s^{-1}) with a correlation coefficient of 0.999 (shown as inset in Fig. 4B), which indicated that the redox process of the prepared bionanocomposites was a surface-confined process. It is well known that flavin adenine dinucleotide (FAD) is deeply embedded in a protective protein shell, which makes the direct electron communication with electrodes extremely difficult. Therefore, MWNTs might facilitate an electron transfer process between the GOD and the electrode substrate.

MWCNTs can facilitate the direct electron transfer of GOD, as shown in the early report (Cai and Chen, 2004), due to their small dimension, electronic structure, high electrical conductivity and some groups containing oxygen on the surface. To verify the advantage of MWCNTs/PSS/Au-IL nanocomposites for GOD conjugation, two control experiments were undertaken. For this purpose, MWCNTs/PSS and MWCNTs/PSS/IL were modified onto GC electrodes by the same method to examine the immobilization of GOD. The

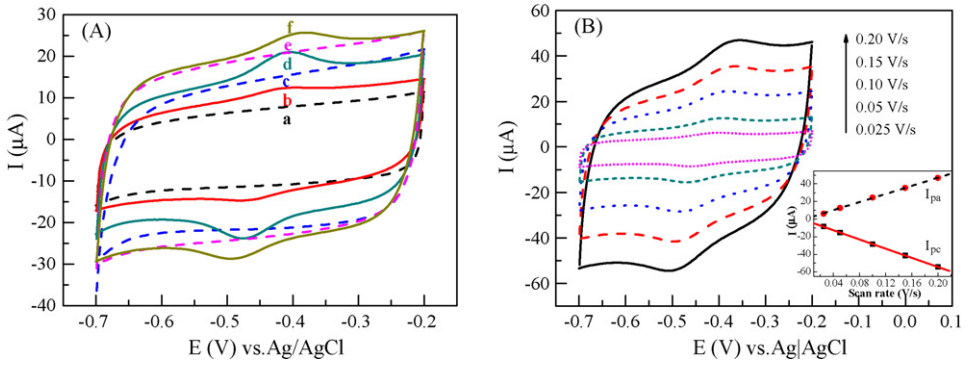

Fig. 4. CV grams (A) at (a) MWCNTs/PSS- (b) MWCNTs/PSS/GOD- (c) MWCNTs/PSS/IL- (d) MWCNTs/PSS/IL/GOD- (e) MWCNTs/PSS/Au-IL- (f) MWCNTs/PSS/Au-IL/GOD-modified GC electrodes in 0.05 M N_2-saturated PBS (pH 7.0) solution at a scan rate of 0.05 V s^{-1}; (B) at MWCNTs/PSS/Au-IL/GOD electrode in 0.05 M N_2-saturated PBS solution at various scan rates. Scan rate: 0.025, 0.05, 0.10, 0.15 and 0.20 V s^{-1} from inner to outer. Inset is the calibrated plot of peak currents vs. scan rates.

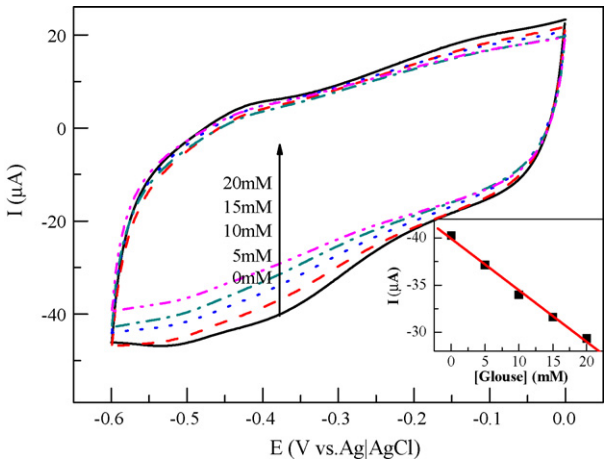

Fig. 5. CV grams at MWCNTs/PSS/Au-IL/GOD-modified GC electrode in various concentrations of glucose PBS solution (pH 7.0) saturated with O_2: 0, 5, 10, 15, and 20 mM from outer to inner. Inset is the calibration curve corresponding to amperometric responses. Scan rate: 0.05 V s^{-1}.

redox behavior, possibly derived from the direct electron transfer of GOD could also be observed at such a MWCNTS/PSS-modified GC electrode (Fig. 4A, curves a and b), but this redox waves were not obvious as that of MWCNTs/PSS/IL (Fig. 4A, curves c and d) and MWCNTs/PSS/IL-Au-modified (Fig. 4A, curves e and f) electrodes.

IL-NH_2 on the surface of MWCNTs/PSS might play an additionally delicate role in the effective immobilization of GOD on MWCNTs/PSS through ionic interaction. As known, GOD is net negatively charged in the pH 7.0 solution, and MWCNTs/PSS was also negatively charged, hence the electrostatic repulsion between the two was against the physical absorption of GOD. In contrast, the IL unit (imidazolium cation) was positively charged. Moreover, Br^- anion in MWCNTs/PSS/IL was ready to be exchanged (Zhang et al., 2006). Therefore, the ionic interaction provided an extra ionic affinity between MWCNTs/PSS and GOD, which is helpful for the immobilization of GOD on MWCNTs/PSS. Moreover, IL-NH_2 has large quantities of amido groups which can form strong interaction between the enzyme and the nanocomposites. The enzyme is able to be physically entrapped into the MWCNTs/PSS/Au-IL nanocomposites. Therefore, MWCNTs/PSS/Au-IL nanocomposites might facilitate the electron transfer process between the GOD and the electrode substrate.

As a result of the presence of Au nanoparticles, an obvious increase in the background current was observed, and the anodic peak and cathodic peak were all increased, which indicated that Au-IL-modified MWCNTs/PSS was much favorable for the immobilization of GOD because of its rough surface confirmed by Raman measurements.

The achieving direct electron transfer of redox enzyme and maintaining its substrate specific enzyme activity are both important for biosensorics and bioelectronics. If the bioactivity of immobilized GOD is retained, the integrated bionanocomposites can be used further, as an example, to fabricate a glucose sensor. Fig. 5 shows the CV grams at MWCNTs/PSS/Au-IL/GOD-modified GC electrode in O_2-saturated PBS solution with various concentrations of glucose. The peak current originating from reduction of O_2 and H_2O_2 became smaller with the increase of the glucose concentrations (Zhang et al., 2007), which should conclude that the specific enzyme–substrate activity of GOD has been reserved in the MWCNTs/PSS/Au-IL/GOD bionanocomposites (as shown in this Fig. 5). Moreover, the calibration curve corresponding to amperometric responses (shown as inset in Fig. 5) is linear vs. the concentrations of glucose ranging from 0 to 20 mM with a correlation coefficient of 0.997. It provided us a potential application of such a bionanocomposite in electrochemical detection of glucose.

The fabrication reproducibility of five electrodes, made independently under the same conditions, showed an acceptable reproducibility with a R.S.D. of 4.8% for the current determined at 5 mM glucose concentrations. The operational stability of the enzyme electrode was measured by a same enzyme electrode's continuous response to 0.05 M PBS containing 5 mM glucose. There is 1.6% relative standard deviation for five times continuous determinations. The storage stability of the biosensor was also studied. When not in use, the biosensor was stored dry at 4 °C. The stability of the glucose biosensor was investigated by monitoring the biosensor response with 5 mM glucose every day for 1 week. The response current of the biosensor decreased by 10.3% after 1 week (7 times) measurements. The good stability of the biosensor can be attributed to two reasons: first, the enzyme is physically entrapped in the MWCNTs/PSS/Au-IL nanocomposite, which has large quantities of amido groups from IL-NH_2 that are favorable to maintain the activity of the enzyme, can form strong interaction between the enzyme and the composites; second, Au nanoparticles has some biocompatibility which offer a more friendly environment for GOD immobilization.

4. Conclusions

In sum, we have successfully prepared MWCNTs/PSS/Au-IL nanocomposites via a simple chemical reduction route. The amino group in IL-NH_2 can reduce $HAuCl_4$ solutions to Au nanoparticles, which is also stabilized by such IL-NH_2 component (Au-IL). Simultaneously, the positively charged Au-IL was noncovalently attached to the negatively charged PSS-functionalized MWCNTs based upon the electrostatic interaction. Most gold nanoparticles distributed well on the nanotubes. The composites showed good electrocatalysis toward reduction of oxygen and hydrogen peroxide. And good biocompatibility with glucose oxidase was also demonstrated due to its good biocatalysis toward glucose target, which offered a friendly environment for the immobilization of biomolecules. Duo to its low detection limit, excellent reproducibility, and good stability, such MWCNTs/PSS/Au-IL/GOD bionanocomposites provided us a potential application toward electrochemical detection of glucose.

Acknowledgements

The authors are most grateful to the NSFC, China (No. 20673109), Department of Science and Technology of Jilin Province (Nos. 20080428 and 20080518) and Ministry of Science and Technology (Nos. 2007AA03Z354 and 2007BAK26B06) for their financial support.

Appendix A. Supplementary data

Supplementary data associated with this article can be found, in the online version, at doi:10.1016/j.bios.2008.09.005.

References

Anderson, J.L., Armstrong, D.W., 2005. Anal. Chem. 77, 6453–6462.
Cai, C.X., Chen, J., 2004. Anal. Biochem. 332, 75–83.
Correa-Duarte, M.A., Sobal, N., Liz-Marzán, L.M., Giersig, M., 2004. Adv. Mater. 16, 2179–2184.
Cui, J.B., Daghlian, C.P., Gibson, U.J., 2005. J. Phys. Chem. B 109, 11456–11460.
Cui, R.J., Huang, H.P., Yin, Z.Z., Gao, D., Zhu, J.-J., 2008. Biosens. Bioelectron. 23, 1666–1673.
Deng, C.Y., Chen, J.H., Chen, X.L., Xiao, C.H., Nie, L.H., Yao, S.Z., 2008. Biosens. Bioelectron. 23, 1272–1277.
Gholap, A.R., Venkatesan, K., Daniel, T., Lahoti, R.J., Srinivasan, K.V., 2003. Green Chem. 5, 693–696.

Han, L., Wu, W., Kirk, F.L., Luo, J., Maye, M.M., Kariuki, N.N., Lin, Y.H., Wang, C.M., Zhong, C.J., 2004. Langmuir 20, 6019–6025.
Harris, P.J.F., 2004. Int. Mater. Rev. 49, 31–43.
Iijima, S., 1991. Nature 354, 56–58.
Itoh, H., Naka, K., Chujo, Y., 2004. J. Am. Chem. Soc. 126, 3026–3027.
Jamróz, D., Maréchal, Y., 2005. J. Phys. Chem. B 109, 19664–19675.
Jaramillo, T.F., Baeck, S.-H., Cuenya, B.R., McFarland, E.W., 2003. J. Am. Chem. Soc. 125, 7148–7149.
Jiang, H.J., Zhu, L.B., Moon, K.-s., Wong, C.P., 2007. Carbon 45, 655–661.
Jiang, K.Y., Eitan, A., Schadler, L.S., Ajayan, P.M., Siegel, R.W., Grobert, N., Mayne, M., Reyes-Reyes, M., Terrones, H., Terrones, M., 2003. Nano Lett. 3, 275–277.
Jiang, L., McNeil, C.J., Cooper, J.M., 1995. J. Chem. Soc., Chem. Commun., 1293–1295.
Kim, D.S., Lee, T., Geckeler, K.E., 2006. Angew. Chem. Int. Ed. 45, 104–107.
Kim, S.J., Park, Y.J., Ra, E.J., Kim, K.K., An, K.H., Lee, Y.H., Choi, J.Y., Park, C.H., Doo, S.K., Park, M.H., Yang, C.W., 2007. Appl. Phys. Lett. 90 (023114), 1–3.
Lee, S.-g., 2006. Chem. Commun., 1049–1063.
Liu, Z., Sun, X.M., Nakayama-Ratchford, N., Dai, H.J., 2007. ACS Nano 1, 50–56.
Mehnert, C.P., Cook, R.A., Dispenziere, N.C., Afeworki, M., 2002. J. Am. Chem. Soc. 124, 12932–12933.
Musameh, M.M., Kachoosangi, R.T., Xiao, L., Russell, A., Compton, R.G., 2008. Biosens. Bioelectron. 24, 87–92.
O'Connell, M.J., Bachilo, S.M., Huffman, C.B., Moore, V.C., Strano, M.S., Haroz, E.H., Rialon, K.L., Boul, P.J., Noon, W.H., Kittrell, C., Ma, J.P., Hauge, R.H., Weisman, R.B., Smalley, R.E., 2002. Science 297, 593–596.
O'Connell, M.J., Boul, P., Ericson, L.M., Huffman, C., Wang, Y.H., Haroz, E., Kuper, C., Tour, J., Ausman, K.D., Smalley, R.E., 2001. Chem. Phys. Lett. 342, 265–271.
Park, M.J., Lee, J.K., Lee, B.S., Lee, Y.-W., Choi, I.S., Lee, S.-g., 2006. Chem. Mater. 18, 1546–1551.
Schäfer, T., Di Paolo, R.E., Franco, R., Crespo, J.G., 2005. Chem. Commun., 2594–2596.
Shen, Y.F., Zhang, Y.J., Qiu, X.P., Guo, H.Q., Niu, L., Ivaska, A., 2007. Green Chem. 9, 746–753.
Smith, J.L., Herman, R.G., Terenna, C.R., Galler, M.R., Klier, K., 2004. J. Phys. Chem. A 108, 39–46.
Tatumi, R., Fujihara, H., 2005. Chem. Commun., 83–85.
Wang, F., Wang, G.C., Yang, S., Li, C.Z., 2008. Langmuir 24, 5825–5831.
Wildgoose, G.G., Banks, C.E., Compton, R.G., 2006. Small 2, 182–193.
Wu, B.Y., Hou, S.H., Yin, F., Zhao, Z.X., Wang, Y.Y., Wang, X.S., Chen, Q., 2007. Biosens. Bioelectron. 22, 2854–2860.
Xue, B., Chen, P., Hong, Q., Lin, J.Y., Tan, K.L., 2001. J. Mater. Chem. 11, 2378–2381.
Zhang, J., Wang, G.L., Shon, Y.-S., Zhou, O., Superfine, R., Murray, R.W., 2003. J. Phys. Chem. B 107, 3726–3732.
Zhang, Y.J., Shen, Y.F., Han, D.X., Wang, Z.J., Song, J.X., Li, F., Niu, L., 2007. Biosens. Bioelectron. 23, 438–443.
Zhang, Y.J., Shen, Y.F., Yuan, J.H., Han, D.X., Wang, Z.J., Zhang, Q.X., Niu, L., 2006. Angew. Chem. Int. Ed. 45, 5867–5870.